HHS Public Access

Author manuscript

Dev Biol. Author manuscript; available in PMC 2024 May 12.

Published in final edited form as:

Dev Biol. 2023 March ; 495: 35–41. doi:10.1016/j.ydbio.2022.12.004.

The serine/threonine kinase Back seat driver prevents cell fusion to maintain cell identity

Shuo Yang[1], **Aaron N. Johnson**[1,2]

[1]Department of Developmental Biology Washington University School of Medicine St. Louis, MO 63110

Abstract

Cell fate specification is essential for every major event of embryogenesis, and subsequent cell maturation ensures individual cell types acquire specialized functions. The mechanisms that regulate cell fate specification have been studied exhaustively, and each technological advance in developmental biology ushers in a new era of studies aimed at uncovering the most fundamental processes by which cells acquire unique identities. What is less appreciated is that mechanisms are in place to ensure cell identity is maintained throughout the life of the organism. The body wall musculature in the *Drosophila* embryo is a well-established model to study cell fate specification, as each hemisegment in the embryo generates and maintains thirty muscles with distinct identities. Once specified, the thirty body wall muscles fuse with mononucleate muscle precursors that lack a specific identity to form multinucleate striated muscles. Multinucleate body wall muscles do not fuse with each other, which maintains a diversification of muscle cell identities. Here we show the serine/threonine kinase Back seat driver (Bsd) prevents inappropriate muscle fusion to maintain cell identity. Thus, the regulation of cell fusion is one mechanism that maintains cell identity.

Keywords

cell identity; muscle development; myoblast fusion; Bsd; Htl; Jumu

Introduction

Cell fate specification is a hallmark of embryonic development, and as development proceeds fated cells mature and acquire specialized identities and functions. Our understanding of cell fate specification was revolutionized by the gene regulatory network (GRN) hypothesis in which extracellular signals regulate the expression of transcription factors that in turn regulate gene expression via *cis*-regulatory modules in the network, establish cell identity, and ultimately activate expression of structural genes (Peter and Davidson, 2016). Cell identity is intimately connected to the overall body plan, and maintenance of cell identity ensures cell type specific functions continue to operate. One

[2]Author for correspondence: anjohnson@wustl.edu.

Author Contributions. Conceptualization: S.Y. and A.N.J., Methodology: S.Y. and A.N.J., Formal analysis: S.Y. and A.N.J., Investigation: S.Y., Resources: A.N.J.; Data curation: S.Y., Writing original draft: S.Y. and A.N.J.

Competing interests. The authors declare no competing interests.

mechanism that promotes the stability of cell identity involves epigenome regulated changes in the accessibility of chromatin to transcription factors (Balsalobre and Drouin, 2022). However, the genomes of neighboring cells must remain isolated for epigenomics to maintain cell identity.

After gastrulation, the *Drosophila* mesoderm subdivides into the cardiac, visceral and somatic mesoderm, and the somatic mesoderm will give rise to the striated body wall muscles. Thirty distinct body wall muscles develop per hemisegment, and each muscle expresses a distinct set of transcription factors that confers a unique cell identity. The diversification of body wall muscle cell types initiates when Wingless and Decapentaplegic signals establish competence domains in the somatic mesoderm (Carmena et al., 1998). Cells in each competence domain are able to respond to Receptor Tyrosine Kinase (RTK) signals, and the cells that transduce the highest amount of RTK signals will form a smaller equivalence group of cells that are able to differentiate into a founder cell (FC). Lateral inhibition within the equivalence group selects a single progenitor to become a FC. The remaining cells in the equivalence group will become fusion competent myoblasts (FCMs). Altogether, thirty FCs are specified per hemisegment and each FC acquires a unique identity that is maintained by the expression of a combinatorial code of transcription factors known as identity transcription factors (de Joussineau et al., 2012; Sandmann et al., 2006). Thus muscle cell identity and diversification depends on the restricted expression of identity transcription factors to subsets of founder cells.

FCs fuse with FCMs and mature into multinucleate founder myotubes (FMTs), but FCs and FMTs will not fuse with each other (Bothe and Baylies, 2016). Once initiated, FMT-FCM fusion can continue as the FMT elongates and attaches to muscle attachment sites on tendon cells (Yang et al., 2022). By the completion of myogenesis, the thirty FMTs will have matured into thirty contractile body wall muscles with distinct identities, morphologies, and intrasegmental positions. Establishing the stereotypical body wall muscle pattern depends on FC diversification to be maintained in FMTs, which is accomplished in part by preventing FMT-FMT fusion.

Here we report that the serine/threonine kinase Back seat driver (Bsd) prevents FMT-FMT fusion. Live imaging studies revealed multinucleate FMTs myotubes can fuse with each other in the absence of Bsd activity. Mechanistically, we had shown that Bsd and the Rho GTPase Tumbleweed (Tum) function in a common pathway to regulate muscle morphogenesis (Yang et al., 2022), but Tum does not appear to regulate FMT-FMT fusion. Instead Bsd regulates the expression of the myoblast fusion *kirre*, which may be a mechanism for limiting FMT-FMT fusion. We used a computational approach to identify regulators of Bsd activity, and found the transcription factor Jumeau (Jumu) activates *bsd* expression. Jumu also regulates the expression of *heartless* (*htl*), which encodes a Fibroblast Growth Factor receptor that directs FMT morphogenesis (Yang et al., 2020). Our studies suggest that Jumu directs body wall muscle morphogenesis by regulating *bsd* and *htl* expression.

Results and Discussion

Bsd prevents myotube fusion

Founder myotubes (FMTs) elongate just after specification, and concurrently fuse with neighboring fusion competent myoblasts (FCMs) to form syncytial myotubes (Bothe and Baylies, 2016). In wild-type embryos, FMT leading edges navigate across the hemisegment and identify muscle attachment sites on tendon cells in the ectoderm. Myotube guidance refers to the combined processes of leading edge navigation and muscle attachment site selection (Yang et al., 2020), and regulated myotube guidance establishes a stereotypical musculoskeletal pattern in abdominal segments A2-A8 (Figure 1A).

Each FMT expresses a combinatorial code of transcription factors known as identity genes (Fig. 1B)(de Joussineau et al., 2012; Tixier et al., 2010). Enhancers from the identity gene *slouch* (*slou*) were used to generate a transgenic reporter gene (*slou-CD8-GFP*) that is active in six FMTs that give rise to the Dorsal Transverse 1 (DT1), the Longitudinal Oblique 1 (LO1), Ventral Acute 1–3 (VA1–3), and the Ventral Transverse 1 (VT1) muscles (Figure 1A)(Schnorrer et al., 2007). A transgenic *Gal4* line constructed from similar *slou* enhancers (*slou.Gal4*) recapitulates the activity of the *slou-CD8-GFP* reporter (Yang et al., 2020). Enhancers from the identity gene *nautilus* (*nau*) comprise a third transgenic line (*nau.Gal4*), which is active in the Dorsal Oblique 3 (DO3), Longitudinal Lateral 1 (LL1), Ventral Lateral 1 (VL1), and Ventral Oblique 4–5 (VO4–5; Fig. 1A)(McAdow et al., 2022). GFP and tdTomato from the *slou-CD8-GFP* and *nau.Gal4, UAS.tdTomato* (*nau>tdTom*) transgenes are rarely co-expressed in wild-type FMTs. We identified Back seat driver (Bsd) in a screen for regulators of myotube guidance (Yang et al., 2022), and found the number of FMTs that co-expressed GFP and tdTomato was significantly greater in bsd^1 embryos than in wild-type embryos (Fig. 1C,D). These observations suggested body wall muscles in bsd^1 embryos adopt hybrid identities.

We used live imaging to understand how Bsd regulates muscle identity. *slou.Gal4, UAS.GFP* (*slou>GFP*) embryos express GFP in six FMTs per hemisegment, and during myotube guidance wild-type *slou>GFP* FMTs did not fuse with each other (Fig. 1E, Supplementary Movie 1). However, in bsd^1 embryos, 28% of *slou>GFP* positive LO1 FMTs fused with *slou>GFP* DT1 FMTs, and 17% of *slou>GFP* positive VT1 FMTs fused with *slou>GFP* VA1 or VA2 FMTs (Fig. 1E,F, Supplementary Movie 1). We did not observe *slou>GFP* FMTs crossing segment borders in bsd^1 embryos, suggesting FMTs within a hemisegment inappropriately fused. The fusion of LO1 and DT1 FMTs is predicted to generate a muscle cell with hybrid identity (LO1-DT1). Similarly, the fusion of VT1 with VA1/VA2 FMTs could produce muscle cells with hybrid identities. Our live imaging studies argue Bsd prevents FMT-FMT fusion to ensure thirty unique muscles develop per hemisegment.

Bsd regulates ERK activity

Bsd directly activates Polo kinase, and active Polo in turn regulates downstream effectors, including the GTPase activating protein Tumbleweed (Tum) and the kinesin microtubule motor protein Pavarotti (Pav) (D'Avino et al., 2006; Ebrahimi et al., 2010; Gregory et al., 2008; Somers and Saint, 2003; Yang et al., 2022). Polo, Tum, and Pav act in a common

myogenic pathway to direct myotube guidance (Guerin and Kramer, 2009; Yang et al., 2022), so we asked if Bsd acts through the Polo/Tum/Pav pathway to prevent FMT-FMT fusion. *tum*^{DH15} produced the strongest myotube guidance phenotypes among the *polo*, *pav*, and *tum* alleles we characterized (Yang et al., 2022), but LO1 myotubes did not fuse with neighboring *slou>GFP* myotubes in *tum*^{DH15} embryos (Fig 2A,B; Supplementary Movie 2). These data argue Bsd acts through a Polo/Tum/Pav independent pathway to regulate FMT fusion.

To identify the mechanism by which Bsd prevents FMT-FMT fusion, we considered additional pathways that Bsd might regulate. The Bsd orthologue Vaccinia-related kinase 3 (VRK3) modulates activity of the extracellular signal-regulated kinase (ERK) by regulating the ERK phosphatase Vaccinia H1-related (VHR)(Kang and Kim, 2006, 2008). In embryonic visceral muscles ERK activates the expression of *kirre*, which encodes a cell adhesion protein that is essential for myoblast fusion (Englund et al., 2003; Krauss, 2010). One possibility is that Bsd inactivates ERK to reduces *kirre* expression and prevent FMT-FMT fusion. We assayed phosphorylated ERK (dpERK) *in vivo* and *in vitro*, and found *bsd*^{1} embryos had significantly more dpERK than control embryos (Fig. 2C,D), and S2 cells transfected with Bsd had significantly less phosphorylated ERK than control transfected cells (Fig. 2E). In addition, embryos that overexpressed Bsd in the mesoderm showed reduced *kirre* expression (Fig. 2F). These results are consistent with the hypothesis that Bsd reduces ERK activity to regulate cell fusion.

The transcription factor Jumu activates the expression of *bsd* and *htl*

We next asked how Bsd activity might be regulated during myogenesis. Using mass spectrometry, we identified a number of proteins that physically interact with Bsd, including Polo, but none of the candidates are known regulators of myogenesis (Yang et al., 2022). Regulatory kinases are differentially expressed during organogenesis (Yang et al., 2022), so as an alternative approach to mass spectrometry we used unbiased prediction tools to identify transcription factor binding sites near the *bsd* locus. *bsd* transcription is controlled by two core promoters, and each promoter is less than 400bp from a consensus binding site for the transcription factor Jumeau (Jumu; Fig 3A). Chromatin immunoprecipation and massively parallel DNA sequencing (ChIP-seq) for Jumu in 0–24hr embryos was performed by the modENCODE project (ENCSR946VDB)(Luo et al., 2020). In support of our *in silico* analysis, the ChIP-seq experiment identified a Jumu binding region that overlaps with the *bsd* core promoters (Fig. 3A). By quantitative real time PCR (qRT-PCR) we found *bsd* expression, and the expression of a known Jumu target gene *heartless* (*htl*) (Ahmad et al., 2016), was significantly reduced in *jumu*$^{2.12}$ embryos (Fig. 3B). Consistent with our hypothesis that Bsd reduces *kirre* expression, we found *kirre* transcripts were significantly enriched in *jumu*$^{2.12}$ embryos (Fig. 3B). Jumu is thus a positive regulator of *bsd* and *htl* expression.

Our model of myotube guidance argues Bsd regulates Polo and the microtubule cytoskeleton while Htl transduces FGF signals that regulate the actin cytoskeleton (Yang et al., 2022; Yang et al., 2020). To functionally test the role of Jumu in regulating *bsd* and *htl* expression during myotube guidance, we characterized muscle morphology in *jumu* mutant embryos.

Myotubes in *jumu*$^{2.12}$ embryos were short and incorrectly targeted, which are phenotypes indicative of myotube guidance defects (Fig. 3C,D). In addition *jumu*$^{2.12}$ *bsd*^{1} double mutant embryos showed a more severe phenotype than *jumu*$^{2.12}$ or *bsd*^{1} single mutant embryos (Fig. 3D), which argues Jumu and Bsd participate in multiple pathways to direct myotube guidance. Our mutant analysis is consistent with a model in which Jumu activates *bsd* and *htl* expression to regulate the microtubule and actin cytoskeletons during myotube guidance (Fig. 3E).

The *jumu*$^{2.12}$ allele deletes a majority of the *jumu* coding sequence (Strödicke et al., 2000), but the muscle phenotype in *jumu*$^{2.12}$ embryos was rather weak (Fig. 3D). During cardiac muscle cell specification Jumu and the transcription factor Checkpoint suppressor homologue (CHES-1-like) activate Polo activity through an unknown mechanism (Ahmad et al., 2012). One possibility is that CHES-1-like is functionally redundant to Jumu during myotube guidance. We expect that *jumu ches-1-like* double mutant embryos may show stronger myotube guidance phenotypes and could reveal a role for Jumu and CHES-1-like in preventing FMT-FMT fusion.

Cell fusion and cell identity

The specification of thirty distinct founder cells (FCs) per hemisegment is accomplished through morphogen-induced specification of equivalence groups, lateral inhibition within equivalence groups to establish individual progenitors, and combinatorial expression of distinct transcription factors to generate diverse cell identities. The final musculoskeletal pattern however is established when FCs undergo a morphological transformation into founder myotubes (FMTs), and respond to navigational cues transduced by the transmembrane receptors Heartless, Kon-tiki, and Robo to elongate and identify muscle attachment sites at the segment boundary (Kramer et al., 2001; Schnorrer et al., 2007; Yang et al., 2020). The developmental mechanisms that direct FC cell fate specification and morphogenesis are commonly used strategies that regulate organogenesis across Metazoa, but FMTs also employ a muscle-specific developmental program in which FMTs selectively fuse with mononucleate fusion competent myoblasts (FCMs), but do not fuse with each other (Fig. 1D)(Bothe and Baylies, 2016).

FMT-FCM fusion persists during myotube guidance through a Bsd-dependent mechanism. Myotubes seeded from distinct FCs do not fuse with each other, but in *bsd* mutant embryos unregulated fusion produced muscles with intermediate identities (Fig. 1D). Fusion does not appear to be regulated by the position of a FMT in the segment. *tum* and *htl* myotube leading edges navigate to incorrect positions, but do not fuse with other FMTs (Fig. 2A) (Yang et al., 2020). These observations suggest Bsd prevents myotube fusion by blocking the activity or function of pro-fusion pathways in maturing myotubes. The nephrin-like transmembrane proteins Kirre and Sticks and stones (Sns) are differentially expressed in muscle precursors: Kirre is expressed in FCs and FMTs while Sns is expressed FCMs (Bour et al., 2000; Ruiz-Gómez et al., 2000). Sns is a ligand of Kirre, and heterophilic interactions between Kirre and Sns are thought to confer FC-FCM cell recognition, and provide the adhesive forces necessary for fusion (Krauss, 2010). Homophilic interactions between Kirre expressing cells in culture promotes cell-cell adhesion (Menon et al., 2005), suggesting

enhanced expression or activation of Kirre in myotubes could drive FMT-FMT fusion. *kirre* transcription is induced in visceral muscle cells by ERK signaling (Englund et al., 2003), and we show Bsd negatively regulates ERK activation and *kirre* expression (Fig. 2C–F). It is possible that Bsd suppresses Kirre activity to prevent FMT-FMT fusion and preserve muscle cell identity. However, spatial misexpression of Kirre in the somatic mesoderm alone is not sufficient to induce FMT-FMT fusion (Menon et al., 2005), suggesting Bsd regulates multiple cell fusion proteins during myotube guidance.

Spatiotemporal regulation of kinase expression

The expression of regulatory kinases is spatially and temporally dynamic, and approximately 50% of Drosophila kinases show tissue-specific expression during the late stages of embryogenesis (Yang et al., 2022). Bsd expression follows this pattern, and is enriched in the somatic mesoderm during myotube guidance (Yang et al., 2022). Htl is a receptor tyrosine kinase that transduces FGF signals, and Htl is broadly expressed in the mesoderm after gastrulation (Fisher et al., 2012). However, during organogenesis, *htl* expression is restricted to a subset of progenitors that will give rise to cardiac, somatic, and visceral muscle (Yang et al., 2020). We confirmed that Jumu regulates *htl* expression during myotube guidance, and show Jumu also regulates *bsd* expression (Fig. 3A,B). Jumu is expressed in FCs and, although repressors have been identified that block *jumu* expression in FCMs, the mechanisms that directly activate *jumu* expression in the mesoderm are unknown (Ahmad et al., 2012; Ciglar et al., 2014). We have shown that Jumu dictates the expression of at least two regulatory kinases, Bsd and Htl, which argues only a small number of transcription factors may be needed to establish the dynamic spatiotemporal expression of regulatory kinases that control cell morphogenesis. Since zebrafish regulatory kinases also show dynamic expression patterns (Yang et al., 2022), it will be important to understand how cell identity and the expression of morphogenetic transcription factors like Jumu are coordinated to direct organogenesis across Metazoa.

Methods

Drosophila genetics

The following stocks were obtained from the Bloomington Stock Center: tum^{DH15}, *P{GMR40D04-GAL4}attP2* (*slou.Gal4*), and *P{GMR57C12-GAL4}attP2* (*nau.Gal4*). The other stocks used in this study were bsd^{1} (Yang et al., 2022), $jumu^{2.12}$ (Ahmad et al., 2012), and *P{slou-mCD8-GFP}* (Schnorrer et al., 2007). *Cyo, P{Gal4-Twi}, P{2X-UAS.eGFP}; Cyo, P{wg.lacZ}; TM3, P{Gal4-Twi}, P{2X-UAS.eGFP}; and TM3, P{ftz.lacZ}* balancers were used to genotype embryos.

Immunohistochemistry—Antibodies used were α-Mef2 (1:1000, gift from R. Cripps), α-Tropomyosin (1:600, Abcam, MAC141), α-GFP (1:600, Torrey Pines Biolabs, TP-401), and α-dpERK (1:300, Cell Signaling Technologies, 4377). Embryo antibody staining was performed as described (Johnson et al., 2013); HRP-conjugated secondary antibodies in conjunction with the TSA system (Molecular Probes) were used to detect primary antibodies.

Imaging and image quantification—Embryos were imaged with a Zeiss LSM800 confocal microscope. For time-lapse imaging, dechorionated St12 embryos were mounted in halocarbon oil and scanned at 6min intervals. Control and mutant embryos were prepared and imaged in parallel where possible, and imaging parameters were maintained between genotypes. Fluorescent intensity and cell morphology measurements were made with ImageJ software.

Phenotypic scoring, analysis, and visualization—Each embryonic hemisegment has 30 distinct muscles with a fixed pattern as shown in Figure 1A. Muscle phenotypes were analyzed in hemisegments A2-A7, in a minimum of nine embryos per genotype. A Tropomyosin antibody was used to visualize all body wall muscles, and the percent defective was calculated for each of the 30 muscles in minimum of 42 hemisegments from seven different embryos. % Defective = # of abnormal muscles/hemisegments scored. To visualize affected muscles, percent defective was converted to a schematic heat map on the body wall muscle pattern.

Immunoprecipitation and Western blotting—For *Drosophila* proteins, S2 cells (8×10^6) were transfected with 1.5μg of pAMW.Bsd or pAMW plasmids in 6-well plates. Cells were cultured for 24h collected, washed twice with PBS, lysed with 600μl IP buffer (20 mM Hepes, pH=7.4, 150 nM NaCl, 1% NP40, 1.5 mM $MgCl_2$, 2 mM EGTA, 10 mM NaF, 1 mM Na_3VO_4, 1X proteinase inhibitor), incubated on ice for 30 min, centrifuged at 12000Xg for 15min. The supernatant was collected, and Western blots were performed by standard method using precast gels (#456–1096, BioRad), and imaged with the ChemiDoc XRS+ system (BioRad). Antibodies used for Western blots were α-dpERK (1:1000, Cell Signaling Technologies, 4377), α-ERK (1:1000, Enzo Life Sciences, ADI-KAP-MA001), and α-Myc (1:1000, Sigma, PLA0001).

Quantitative real time PCR—Total RNA was extracted with RNeasy mini kit (74104, Qiagen), and quantified (Nanodrop 2000). cDNA was prepared by reverse transcription with M-MLV Reverse Transcriptase (28025013, Thermo) with 2000ng RNA. PowerUp Sybr Green Master Mix (A25742, Thermo) and ABI StepOne system (Applied Biosystems) were used for quantitative RT-PCR. Quantification was normalized to *GAPDH* or *RpL32*. Primers used:

Htl-F-5`-ACCAAATTGCCAGAGGAATG-3`

Htl-R-5`- GGTAGCCTGCCATTTGTGTT-3`

Bsd- F-5`-TCAACGCTAAGCACTCCGTT-3`

Bsd-R-5`-CGCCTCTGCTCCATGTCTAG-3`

Rp32- F-5`-ATGCTAAGCTGTCGCACAAATG-3`

Rp32- R-5`-GTTCGATCCGATACCGATGT-3`

Bioinformatic and statistical analysis—DNAMAN (Lynnon Biosoft, Ver. 10) was used to identify consensus transcription factor binding sites. Statistical analyses were performed with GraphPad Prism 9 software, and significance was determined with the

unpaired student's t-test, and two-sided Fisher's exact test. Sample sizes are indicated in the figure legends. All individuals were included in data analysis.

Supplementary Material

Refer to Web version on PubMed Central for supplementary material.

Acknowledgements.

We thank Shaad Amhad (Indiana State University) for sending *jumu* flies, and Frank Schnorrer (IBDM, Marseille, France) for providing *slou-mCD8-GFP* flies. We also thank the *Drosophila* community for stocks and reagents, Kevin White's laboratory for performing the Jumu ChIP-seq, and the reviewers for comments that greatly improved the manuscript. ANJ was supported by NIH R01AR070299.

References

Ahmad SM, Bhattacharyya P, Jeffries N, et al. , 2016. Two Forkhead transcription factors regulate cardiac progenitor specification by controlling the expression of receptors of the fibroblast growth factor and Wnt signaling pathways. Development 143, 306–317. [PubMed: 26657774]

Ahmad Shaad M., Tansey Terese R., Busser Brian W., et al. , 2012. Two Forkhead Transcription Factors Regulate the Division of Cardiac Progenitor Cells by a Polo-Dependent Pathway. Developmental Cell 23, 97–111. [PubMed: 22814603]

Balsalobre A, Drouin J, 2022. Pioneer factors as master regulators of the epigenome and cell fate. Nature reviews. Molecular cell biology 23, 449–464. [PubMed: 35264768]

Bothe I, Baylies MK, 2016. Drosophila myogenesis. Current biology : CB 26, R786–791. [PubMed: 27623256]

Bour BA, Chakravarti M, West JM, et al. , 2000. Drosophila SNS, a member of the immunoglobulin superfamily that is essential for myoblast fusion. Genes Dev 14, 1498–1511. [PubMed: 10859168]

Carmena A, Gisselbrecht S, Harrison J, et al. , 1998. Combinatorial signaling codes for the progressive determination of cell fates in the Drosophila embryonic mesoderm. Genes & Development 12, 3910–3922. [PubMed: 9869644]

Ciglar L, Girardot C, Wilczyński B, et al. , 2014. Coordinated repression and activation of two transcriptional programs stabilizes cell fate during myogenesis. Development 141, 2633–2643. [PubMed: 24961800]

D'Avino PP, Savoian MS, Capalbo L, et al. , 2006. RacGAP50C is sufficient to signal cleavage furrow formation during cytokinesis. Journal of Cell Science 119, 4402–4408. [PubMed: 17032738]

de Joussineau C, Bataillé L, Jagla T, et al. , 2012. Diversification of muscle types in Drosophila: upstream and downstream of identity genes. Current topics in developmental biology 98, 277–301. [PubMed: 22305167]

Ebrahimi S, Fraval H, Murray M, et al. , 2010. Polo kinase interacts with RacGAP50C and is required to localize the cytokinesis initiation complex. Journal of Biological Chemistry 285, 28667–28673. [PubMed: 20628062]

Englund C, Lorén CE, Grabbe C, et al. , 2003. Jeb signals through the Alk receptor tyrosine kinase to drive visceral muscle fusion. Nature 425, 512–516. [PubMed: 14523447]

Fisher B, Weiszmann R, Frise E, et al., 2012. BDGP website. https://insitu.fruitfly.org/cgi-bin/ex/insitu.pl.

Gregory SL, Ebrahimi S, Milverton J, et al. , 2008. Cell division requires a direct link between microtubule-bound RacGAP and Anillin in the contractile ring. Current Biology 18, 25–29. [PubMed: 18158242]

Guerin CM, Kramer SG, 2009. RacGAP50C directs perinuclear gamma-tubulin localization to organize the uniform microtubule array required for Drosophila myotube extension. Development 136, 1411–1421. [PubMed: 19297411]

Hao Y, Jin LH, 2017. Dual role for Jumu in the control of hematopoietic progenitors in the Drosophila lymph gland. eLife 6.

Johnson AN, Mokalled MH, Valera JM, et al. , 2013. Post-transcriptional regulation of myotube elongation and myogenesis by Hoi Polloi. Development 140, 3645–3656. [PubMed: 23942517]

Kang TH, Kim KT, 2006. Negative regulation of ERK activity by VRK3-mediated activation of VHR phosphatase. Nature cell biology 8, 863–869. [PubMed: 16845380]

Kang TH, Kim KT, 2008. VRK3-mediated inactivation of ERK signaling in adult and embryonic rodent tissues. Biochimica et biophysica acta 1783, 49–58. [PubMed: 18035061]

Kramer SG, Kidd T, Simpson JH, et al. , 2001. Switching repulsion to attraction: changing responses to slit during transition in mesoderm migration. Science (New York, N.Y.) 292, 737–740. [PubMed: 11326102]

Krauss RS, 2010. Regulation of promyogenic signal transduction by cell–cell contact and adhesion. Experimental Cell Research 316, 3042–3049. [PubMed: 20471976]

Luo Y, Hitz BC, Gabdank I, et al. , 2020. New developments on the Encyclopedia of DNA Elements (ENCODE) data portal. Nucleic acids research 48, D882–d889. [PubMed: 31713622]

McAdow J, Yang S, Ou T, et al. , 2022. A pathogenic mechanism associated with myopathies and structural birth defects involves TPM2 directed myogenesis. JCI Insights 7, e152466.

Menon SD, Osman Z, Chenchill K, et al. , 2005. A positive feedback loop between Dumbfounded and Rolling pebbles leads to myotube enlargement in Drosophila. Journal of Cell Biology 169, 909–920. [PubMed: 15955848]

Peter IS, Davidson EH, 2016. Chapter Thirteen - Implications of Developmental Gene Regulatory Networks Inside and Outside Developmental Biology, in: Wassarman PM (Ed.), Current topics in developmental biology. Academic Press, pp. 237–251.

Ruiz-Gómez M, Coutts N, Price A, et al. , 2000. Drosophila dumbfounded: a myoblast attractant essential for fusion. Cell 102, 189–198. [PubMed: 10943839]

Sandmann T, Jensen LJ, Jakobsen JS, et al. , 2006. A Temporal Map of Transcription Factor Activity: Mef2 Directly Regulates Target Genes at All Stages of Muscle Development. Developmental Cell 10, 797–807. [PubMed: 16740481]

Schnorrer F, Kalchhauser I, Dickson BJ, 2007. The transmembrane protein Kon-tiki couples to Dgrip to mediate myotube targeting in Drosophila. Dev Cell 12, 751–766. [PubMed: 17488626]

Somers WG, Saint R, 2003. A RhoGEF and Rho family GTPase-activating protein complex links the contractile ring to cortical microtubules at the onset of cytokinesis. Developmental cell 4, 29–39. [PubMed: 12530961]

Strödicke M, Karberg S, Korge G, 2000. Domina (Dom), a new Drosophila member of the FKH/WH gene family, affects morphogenesis and is a suppressor of position-effect variegation. Mechanisms of Development 96, 67–78. [PubMed: 10940625]

Tixier V, Bataillé L, Jagla K, 2010. Diversification of muscle types: Recent insights from Drosophila. Experimental Cell Research 316, 3019–3027. [PubMed: 20673829]

Yang S, McAdow J, Du Y, et al. , 2022. Spatiotemporal expression of regulatory kinases directs the transition from mitotic growth to cellular morphogenesis. Nat Commun 13, 772. [PubMed: 35140224]

Yang S, Weske A, Du Y, et al. , 2020. FGF signaling directs myotube guidance by regulating Rac activity. Development 147, dev183624. [PubMed: 31932350]

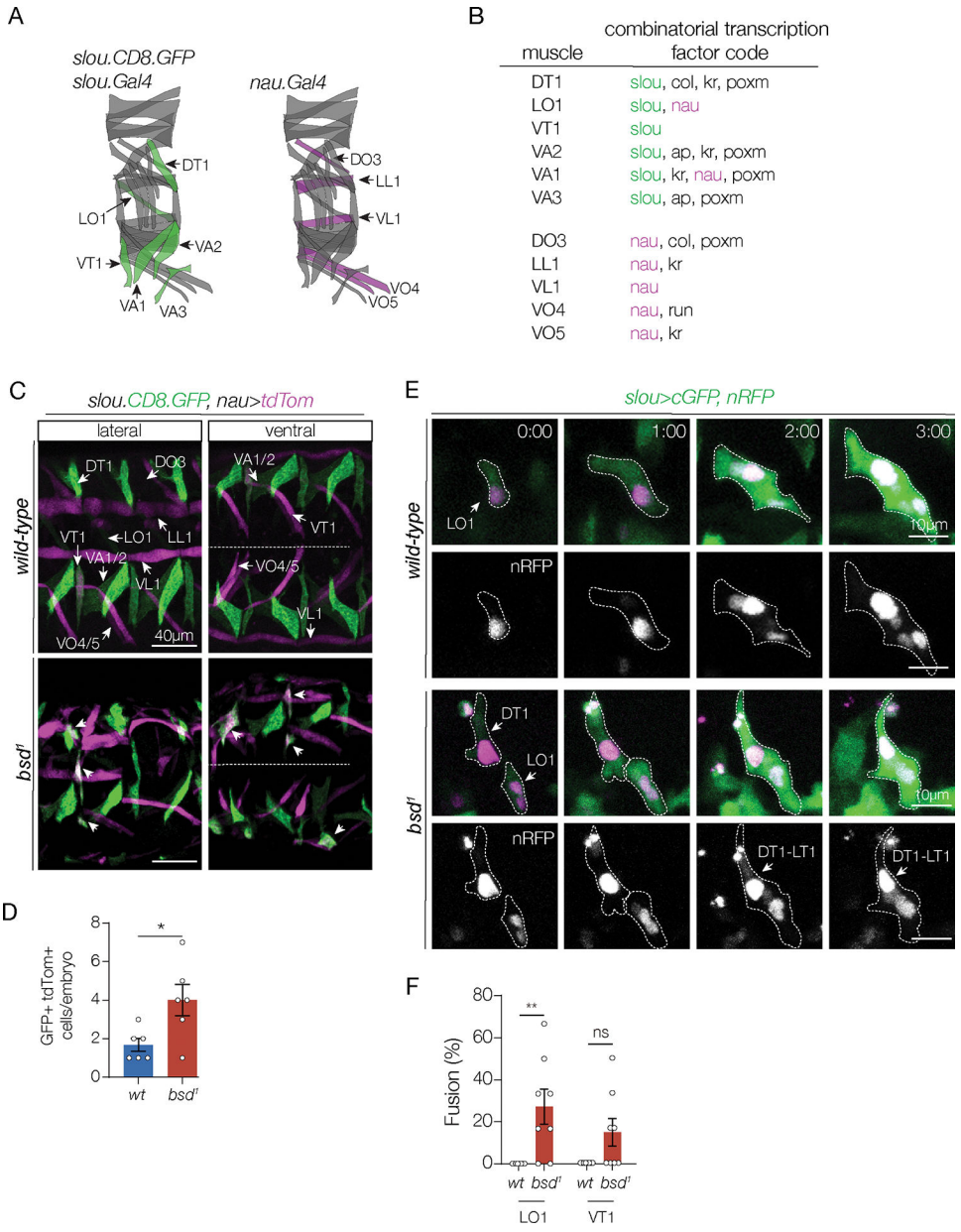

Figure 1. Bsd maintains directional fusion and muscle identity.

(A) Diagrams of the stereotypic pattern of body wall muscles in one hemisegment. Each muscle expresses a unique combination of identity genes, including *slouch* (*slou*) and nautilus (*nau*). *slou* transgenes are active in Doral Transverse 1 (DT1), Longitudinal Oblique (LO1), Ventral Acute 1–3 (VA1–3), and the Ventral Transverse 1 (VT1) muscles (green). A *nau* transgene is active in the Dorsal Oblique 3 (DO3), Longitudinal Lateral 1 (LL1), Ventral Lateral 1 (VL1), and Ventral Oblique 4–5 (VO4–5) muscles (violet). (B) The combinatorial transcription factor code that establishes muscle cell identity as described in (de Joussineau et al., 2012; Tixier et al., 2010). Each muscle expresses a unique set of transcription factors. Note, LO1 is the only muscle that express both *nau* and *slou*, but the *nau.gal4* transgene is not active in LO1 muscle. (C) *bsd*^{1} myotubes

show intermediate identities. Confocal micrographs of live Stage 16 embryos imaged for *slou-CD8-GFP* (green) and *nau>tdTom* (violet). *slou-CD8-GFP* and *nau.Gal4>tdTom* are active in largely non-overlapping populations of body wall muscles in wild-type embryos, although VT1 occasionally co-expressed GFP and tdTom. bsd^{1} embryos had more muscles that co-expressed GFP and tdTom than wild-type embryos (arrowheads). (D) Quantification of GFP/tdTom double positive cells in hemisegments A2-A7; each data point represents one embryo. (E) Multinucleate bsd^{1} myotubes fuse. Live imaging stills of LO1 myotubes in Stage 12–15 embryos that expressed cytoplasmic GFP (green) and nuclear RFP (violet) under the control of *slou.Gal4*. Live imaging initiated when GFP fluorescence was detectable in LO1 myotubes (0:00). Control myotubes elongate in a stereotypical fashion and identify attachment sites to acquire an oblique morphology. Notice the number of LO1 myonuclei increases due to fusion with unlabeled fusion competent myoblasts. bsd^{1} LO1 myotubes often fused with DT1 myotubes and the LO1-DT1 muscle acquired a transverse morphology. (E) Quantification of myotube fusion. The number of LO1 and VT1 fusion events with other *slou>GFP* myotubes in hemisegments A2-A7 is shown; each data point represents one embryo. Significance in (D,F) was determined by unpaired students t-test. Error bars represent SEM. (ns) not significant, (*) $p<0.05$, (**) $p<0.01$. (#:##) hr:min.

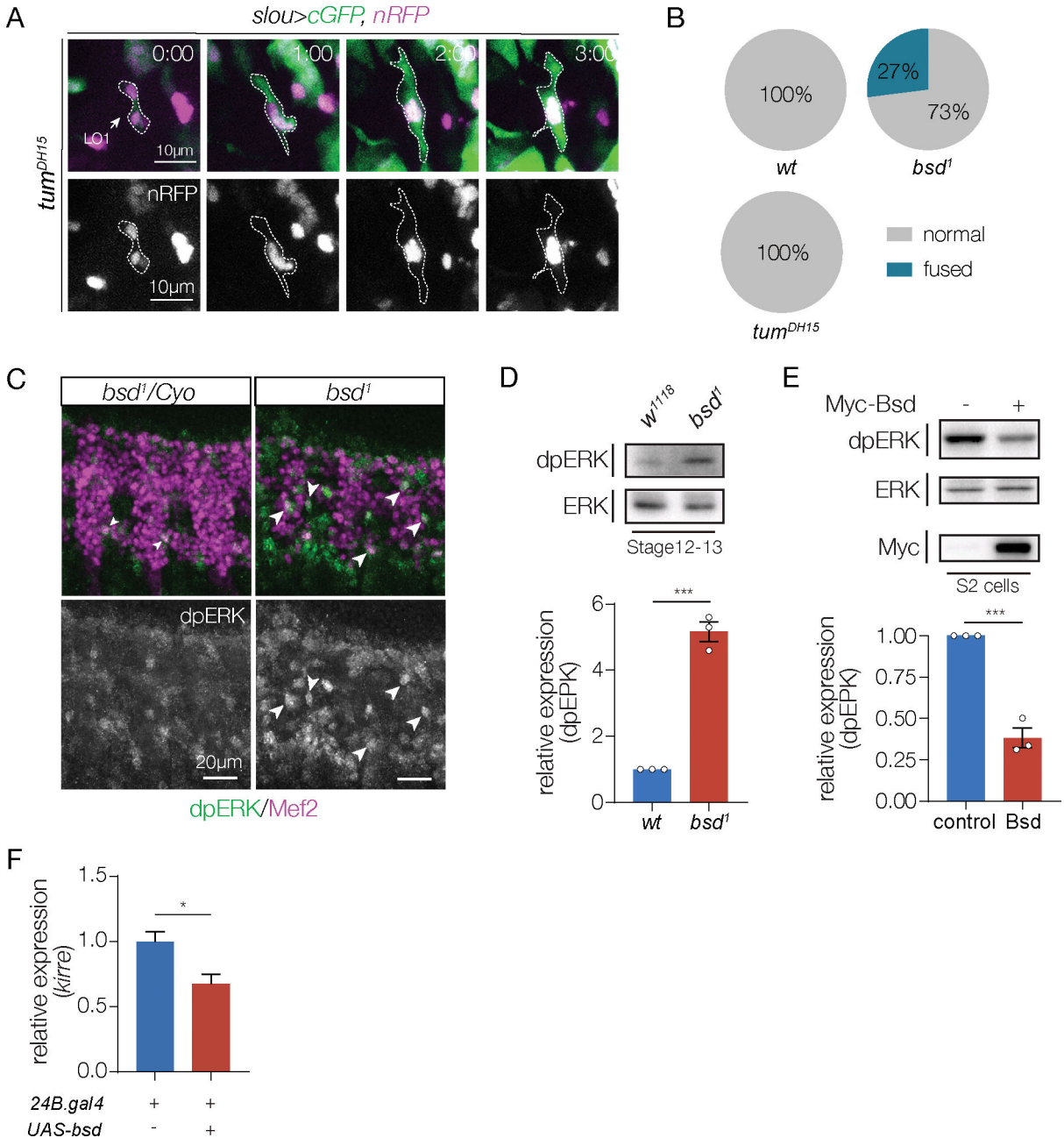

Figure 2. Bsd regulates ERK activity.

(A) Tum does not regulate myotube fusion. Live imaging stills of LO1 myotubes in Stage 12–15 embryos as described in Fig. 1. *tum*^{DH15} LO1 myotubes showed severe guidance defects, but did not fuse with other *slou>GFP* myotubes. (B) Quantification of non-directional myotube fusion from live imaging. n≥6 embryos per genotype. (C-E) Bsd represses ERK phosphorylation. (C) Stage 12 embryos labeled for dpERK (green) and Mef2 (violet). Mef2 is expressed in all myogenic cells. *bsd*^{1} embryos showed more dpERK in the mesoderm than controls. Arrowheads show dpERK/Mef2 double positive cells. (D) Stage 12 embryo lysates immunoblotted with dpERK. *bsd*^{1} embryo lysates showed significantly more phosphorylated ERK than controls. (E) S2 cells transfected with Bsd.Myc

and control plasmids were immunoblotted with dpERK and Myc. Cells transfected with Bsd showed significantly less phosphorylated ERK than controls. Data points in the dpERK quantifications (D,E) represent one biological replicate. (F) Quantitative real time PCR. Stage 12 embryos that overexpressed *bsd* in the mesoderm under the control of *24B.gal4* expressed more *kirre* RNA than control embryos. Significance was determined by unpaired students t-test. Error bars represent SEM. (*) $p<0.05$, (***) $p<0.001$.

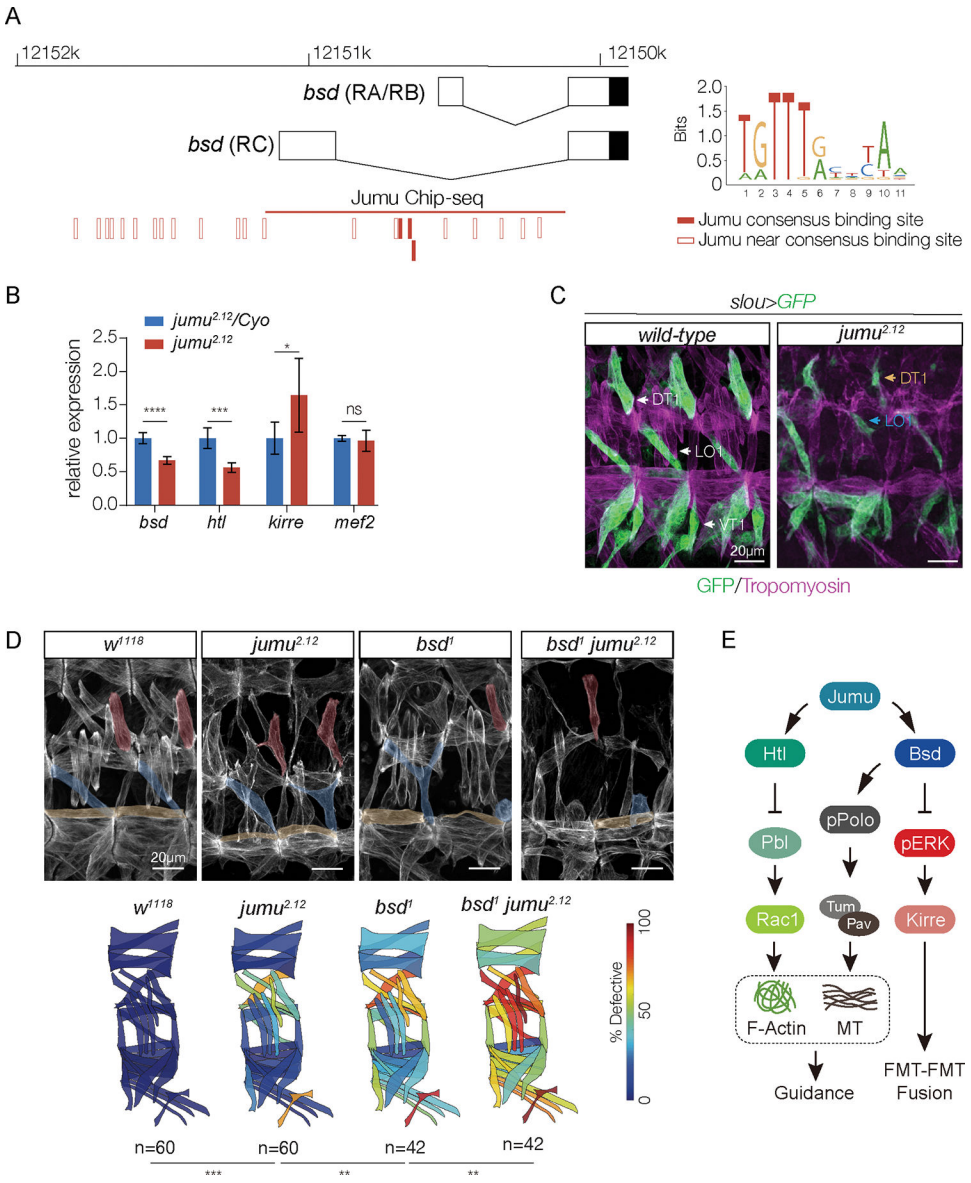

Figure 3. Jumu activates *bsd* expression.

(A) Diagram of the *bsd* core promoter region. Open boxes represent untranslated regions; shaded boxes show the beginning of the open reading frame. Molecular coordinates refer to chromosome 2R. The consensus Jumu binding site was reported in (Hao and Jin, 2017). The ChIP-seq binding region was reported by modENCODE project (ENCSR946VDB). (B) Quantitative real time PCR. Stage 12 *jumu* embryos expressed less *htl* and *bsd* RNA, and more *kirre* RNA than control embryos. *Mef2* expression was unaffected in *jumu* embryos (n=3 biological replicates). (C) *jumu*$^{2.12}$ DT1, LO1, and VT1 muscle phenotypes. Stage 16 embryos labeled for *slou>GFP* (green) and Tropomyosin (violet). *jumu*$^{2.12}$ muscles had attachment site defects (orange and blue arrows). (D) Stage 16 embryos labeled with Tropomyosin. DT1, LO1, and VL1 muscles are pseudocolored red, blue, and yellow. To quantify muscle phenotypes, muscles were scored in hemisegments A2-A7 of Stage 16 embryos as normal or “defective” (missing muscles, muscles with attachment site defects,

and muscles that failed to elongate). The frequencies of muscle defects are shown as a heat map on the stereotypic muscle pattern in one embryonic hemisegment. Muscle morphology defects were more severe in *jumu*$^{2.12}$ *bsd*^{1} double mutant embryos than in *jumu*$^{2.12}$ and *bsd*^{1} single mutant embryos. (n) number of hemisegments scored. (E) Model of myotube guidance and cell fusion pathways. Significance was determined by unpaired students t-test (B) or Fisher's exact test (D). Error bars represent SEM. (*) $p<0.05$, (**) $p<0.01$, (***) $p<0.001$.